International Journal of Life Science Research Archive

ISSN: 0799-6640 (Online)

Journal homepage: https://sciresjournals.com/ijlsra/

(RESEARCH ARTICLE)

Check for updates

The role of gold nanoparticles in anticancer activity

Murtadha M-Hussein A-Kadhim [1,*], Ameer Jawad hadi [2] and Siham Adnan Abdulsada [3]

[1] *Department of Genetic Engineering, College of Biotechnology, AL-Qasim Green University, Ministry of Higher Education and Scientific Research, Iraq*
[2] *Department of Medical Biotechnology, AL-Qasim Green University, Ministry of Higher Education and Scientific Research, Iraq*
[3] *Directorate education babil, Iraq.*

International Journal of Life Science Research Archive, 2023, 05(01), 019–028

Publication history: Received on 01 May 2023; revised on 15 June 2023; accepted on 18 June 2023

Article DOI: https://doi.org/10.53771/ijlsra.2023.5.1.0064

Abstract

To enhance the cellular uptake and chemotherapeutic efficacy of a current chemotherapeutic medication, a nanoparticle drug carrier technology has been designed. Due to their distinctive electrical and optical characteristics, gold nanoparticles (Au NPs) have recently demonstrated intriguing medical and military uses. In the event that they come into touch with a biological system, little is known about their biocompatibility. Metallic nanoparticles have been successfully utilized for a kind of biological applications. A drug delivery system known as Au – PEG – PAMAM – DOX was produced by conjugating the dendrimer with the anti-cancer chemical doxorubicin (DOX) via an amide bond. The amount of DOX released from Au – PEG – PAMAM – DOX at a natural pH was negligible, but this amount significantly increased in an environment with a weak acidic milieu, according to studies on the release of medicines from acellular sources. A research into the intracellular release of the medication was carried out with the assistance of confocal laser scanning microscopy (CLSM). Recently conjugation to the nanosystem, *In vitro* viability experiments revealed an increase in the associated DOX cytotoxicity that could not be attributable to carrier components. This indicates that the effectiveness of the DOX was increased. In light of this, it has been hypothesized that the newly created pH-triggered multifunctional Au NPs- DOX nanoparticle system could pave the way for a viable platform for the intracellular delivery of a range of anticancer medicines. In the current study, the common Au NPs synthesis techniques and their well-established uses in diverse needs, particularly in biological sensing applications.

Keywords: Gold Nanoparticles; Au NPs-DOX; Activity; Anticancer

1 Introduction

Lung cancer, also called lung carcinoma, affects both male and female. It is considered as the leading cause of deaths worldwide [1]. Lung cancer is distinguished into small cell and non-small cell lung cancer based on histologic studies. Generally, an advanced type of non-small cell lung cancer has been thought of as poor prognosis; therefore, new ultimate methods are urgently needed for improving the chances of patient survival [2]. The development of therapies to fight against severely multiplying tumors is very difficult. Numerous treatments are available for cancer therapy but they are restricted by the lack of specificity and dose-limiting toxicity [3]. Finding therapeutic drugs for the treatment of numerous types of cancer is a challenge [4]. However, safest methods are of importance for the combination of controlled release, exhibiting targeted delivery, less harmful, and very effective [5]. Nanomaterials are projected optimistically to develop cancer diagnosis and therapy. Nanotechnology includes the synthesis of nanoscale materials, utilization and understanding of physicochemical and optoelectronic properties. In the new millennium, nanotechnology plays a vital role in the key technologies [6]. Nanoparticles, especially in metal, have obtained great attention because of its distinct physiochemical nature and have become a main active research area due to sensors,

* Corresponding author: Murtadha M-Hussein A-Kadhim

imaging, cosmetics, and cancer therapy and drug delivery [7]. Gold nanoparticles, (AuNPs) as the best drug nanocarriers, have excellent characteristics with controlled size, stability, and biocompatibility, which makes them potential agent in cancer diagnosis and treatment [8]. They are employed to visualize the tumors in their primary-secondary locations and can also be used as delivery vehicles for the anticancer drug [9]. Gold nanoparticles are the most gorgeous nanomaterials for diverse applications like catalytic, anticancer, antimicrobial, anti-inflammation, and various biomedical research [10]. created a gold nanoparticle - based drug delivery nanosystem to modulate the intracellular drug release of DOX *In vitro* via an increased permeability and retention (EPR) effect. Owing to their biocompatibility and unique optical, physical, and electrical properties, gold nanoparticles are widely employed in biomedical nanotechnologies for targeted drug delivery [11-12]. It has also been revealed that the intracellular drug delivery location can be tracked using 4, surface enhanced Raman scattering due to the surface plasmon resonance properties of the Au NPs (SERS) [13-14]. Au nanoparticles are frequently treated with polymers such as poly (ethylene glycol) (PEG) to increase its stability without affecting its biocompatibility, while simultaneously enhancing its potential for biomedical applications [15-16]. In generally, the inclusion of the PEGpolymer is known to increase the electrostatic repulsion between nanoparticles, hence enhancing the stability of colloidal Au NPs [17]. It has also been shown that connecting aPEGpolymer to Au nanoparticles improves there in vivo accumulation at tumor sites by prolonging the nanoparticles' circulation lifetime. [18]. Hence, PEG conjugation on the surface of spherical Au nanoparticles may assist minimize deleterious effects and reduce their uptake during bloodstream circulation by the reticuloendothelial system (RES) [19-20]. The drug loading capacity of nanoparticles determines the over all efficacy of drug delivery systems. Dendrimers can be used to conjugate pharmaceuticals and targeting ligands at the same time, and their structures have the potential to boost drug loading capacity due to their highly branching nature, 3-D spherical morphology, surface multi-functionality, and well-defined composition [21-22]. As a chemotherapeutic smart drug delivery system, we describe a new pH - responsive PEGylated dendrimer modified drug coupled Au NPs. Data on the combined use of a PEGpolymer and polyamido amide (PAMAM) dendrimers with doxorubicin for cancer therapy are currently rare in the scientific literature, and *In vitro* interactions are only mentioned briefly. [23-24]. Huang et al. investigated the intracellular activity of nanoparticles using confocal laser scanning microscopy (CLSM) in order to develop nanoparticle-based drug delivery devices [25-26]. [27] Photo thermal- chemotherapy with 5PEGylated dendrimer-doxorubicin linked gold nano rods was described. This system requires a linker to conjugate doxorubicin in five steps; however, the nanosystem was synthesized in four steps using a modified PEG as a stabilizing agent instead of a linker in the current study. The construction of the drugdelivery vehicle $Au - PEG - PAMAM - DOX$ conjugate and the tracking of intracellular In this paper, drug release using confocal laser scanning microscopy (CLSM) pictures is reported.

2 Material and methods

2.1 Materials and Chemicals

Trisodium citrate dehydrate, 1- ethyl - 3 - (3-dimethylaminopropyl) carbodimide hydrochloride, N-hydroxysulfosuccinimide, and gold (III) chloride trihydrate (HAuCl4.3H2O) (NHS) were purchased from SantaCruz of Biotechnology. PAMAM dendrimer succinamic acid 10% in water solution was purchased from Sigma, diisopropyl ethylamine (DIPEA) and doxorubicin hydrochloride DOX were purchased from Santa Cruz of Biotechnology. Cell culture media Dulbecco's Modified Eagle Medium (DMEM). All supplements, Fetal Bovine Serum (FBS), L-Glutamine, Streptomycin, trypsin from Sigma.

2.2 Synthesis and characterization of AuNPs

In a brief, a solution containing 1 mM HAuCL4.3H2O was brought to a boil in 100 ml of water while being rapidly agitated throughout the process. Following this, 10 ml of 40.0 mM sodium citrate was added to the mixture. As a result, the solution's color changed from light yellow to deep red. After 10 minutes of continuous boiling, the heating was turned off, and the solution was agitated for a further 15 minutes [11]. The created nanoparticles were kept in a freezer at 4 ºC. until needed.

2.3 PEG thiol loading with AuNPs

In order to functionalize the Au NPs, 1 mM of SHPEG-NH2 (MW 5 kDa) was added to a 30 μM of 70 ml Au NPs solution, and the mixture was agitated for an additional 15 minutes. The mixture was then left to react at 4 ºC. overnight [12]. After that, the unreacted PEG was separated from the solution by employing a dialysis membrane with a MWCO of 30 kDa. The sample was then washed three times with ultrapure water, and the purified product was stored at a temperature of 4 ºC.

2.4 PAMAM banding with Au-PEG

A water solution of $PAMAM - COOH$ (2 ml containing 2 mg), $EDC.HCl$ (1.78 mg), and NHS (1 mg) was added to the $Au - PEG\ NPs$ in order to cause a change in their structure. In order to activate the carboxylic group of PAMAM, the mixture was agitated for a period of thirty minutes while the temperature was maintained at room temperature. The $Au - PEG\ NPs$ solution (50 ml, 14 µM AuNPs conc.) was agitated for an additional 48 hours after the addition of this solution [13-14]. The solution was then dialyzed one more time using a dialysis membrane (MWCO 30 kDa) and the temperature was maintained at 4 ºC in order to eliminate any unreacted PAMAM.

2.5 DOX loading to Au-PEG-PAMAM NPs

After mixing the produced $Au - PEG - PAMAM\ NPs$ (30 ml) at 0 ºC for five minutes, the following steps were carried out : the addition of HBTU (3.5 mg) and DIPEA (4.31µl) was followed by an additional ten minutes of stirring. A solution of doxorubicin (1 ml containing 2 mg) was then added to the mixture, and the reaction was stirred for forty-eight hours at room temperature without being exposed to light from the outside [15]. The completed product was then dialyzed once more over a dialysis membrane with a MWCO of 30 kDa to eliminate any remaining free DOX before being stored at 4 ºC.

2.6 Drug loading efficiency

The drug loading efficiency was estimated using a direct method based on the absorption of the DOX at 480 nm. In brief, the nano-carrier system's unknown drug concentration was calculated using a calibration curve based on a series of known DOX values. The drug loading efficiency was then determined using the equation (1)

Amount of drug in micelle

$$Loading\ efficiency\ \% = \frac{mount\ of\ drug\ in\ micelle}{otal\ amount\ of\ drug\ in\ feed} \times 100\% \ldots\ldots (1)$$

Total amount of drug in feed.

2.7 Physicochemical characterization of drug delivery system

Using a Spectra Max M3 multi - mode microplate reader, observations of fluorescence at 471 nm and absorption at 480 nm. were performed (Molecular Devices, USA). Using the Zetasizer nanoanalyzer, the hydrodynamic size, poly dispersity index (PDI), and zeta potentials of the nanoparticles were determined (Malvern Instruments, Worcestershire, UK). The Hitachi SU 6600 FESEM apparatus was used for scanning electron microscopy (SEM) analysis. The SEM were created by spinning the nanoparticle solution at 1000 rpm for 20 seconds on prewashed silicon substrates and drying them in air in a dust-free environment. Transmission electron microscopy (TEM) investigation was performed on an FEI Tecani F30 with a 300 kV accelerating voltage. The TEM pictures were created by a drop of material evaporating in air at ambient temperature on a coated 400 mesh copper grid. The point resolution in TEM mode is 0.19 nm. With the use of a Zeiss 510 laser scanning microscope, confocal images were taken (Oberkochen, Germany).

2.8 Cell culture

The A549 cell line (human lung cancer) was obtained from Santa Cruz and grown in DMEM media supplemented with 10% FBS, 45 IUml-1 penicillin and 45 $IU\ ml\ -\ 1$ streptomycin in a humidified 5% $CO2$ incubator at 37 ^{o}C.

3 Results and discussion

3.1 Synthesis and Characterization of $Au - PEG - PAMAM - DOX$

As mentioned earlier, we generated a pH-sensitive $\boldsymbol{Au - PEG - PAMAM - DOX}$ The purpose of this nano system is to modify the cellular absorption process and enhance the efficacy of DOX treatment at acidic cancer locations. A PEGylated Au sphere PAMAM polymeric conjugate was synthesized using a manufacturing method that included multiple stages.By reducing gold chloride with citrate, Au NPs were made. CN, NH2, and SH are all examples of polymer functional groups that can be employed to stabilize Au through the formation of covalent bonds. These groups are extremely attractive to Au NPs. In order to further improve the citrate-capped Au'NPs resistance to hydrolysis, a thiolated PEG polymer was later applied to their surface. The biocompatibility of nanoparticles can be improved by coating the surface of the particles with dendrimer molecules. Following the application of PEG for stabilization, the surface of the Au NPs was modified with a carboxylated PAMAM polymeric matrix using an EDC coupling process. This procedure involved

the formation of an amide bond between the dendrimer and the amine group of the PEG polymer. In the final step an amide bond was formed between the DOX and the carboxylic acid group of the PAMAM by employing DIPEA as a base and HBTU as a coupling agent. This step was necessary for the production of the final $\boldsymbol{Au-PEG-PAMAM-DOX}$ carrier system. In order to confirm the effective conjugation of $\boldsymbol{Au-PEG-PAMAM-DOX}$ dendrimer to AuNPs and drug loading on the nanosystem, a comprehensive characterization of the nanosystem $\boldsymbol{Au-PEG-PAMAM-DOX}$ was performed utilizing UV-Vis absorption spectra. In Figure 1A, The UV-Vis absorption spectra of Au NPs, Au-PEG, Au-PEG-PAMAM, and Au-PEG-PAMAM-DOX are all displayed here for your viewing pleasure. It is common practice to explain the minor change in the nearby surroundings' refractive index to the red shift in the absorbance peak of Au NPs. This change reveals itself as a red shift in the absorbance spectrum. It has been seen that the absorbance spectrum has shifted in this way [27]. As shown in Figure 1A, adding PEG, PAMAM and DOX to the surface of AuNPs caused the longitudinal surface plasmon resonance band to shift to the green by 3 nm, 2 nm, and 2 nm, respectively. This shift can be attributed to the fact that PEG, PAMAM, and DOX are all conjugated on to the surface of AuNPs. PEG, PAMAM, and DOX were successfully conjugated on to the surface of the Au NPs, as evidenced by the differences in the absorbance spectra of the Au NPs, which were regarded as proof. When the 480 nm absorption peak of the DOX in $\boldsymbol{Au-PEG-PAMAM-DOX}$ was compared to a standard curve using absorption spectroscopy, the average loading efficiency was observed to be 45.85% (an average, n = 3 batches) of the DOX that was present in total of the nano- carrier solution. This was determined by taking the average of the results from all three batches. Figure 1b demonstrates this, as may be viewed here.

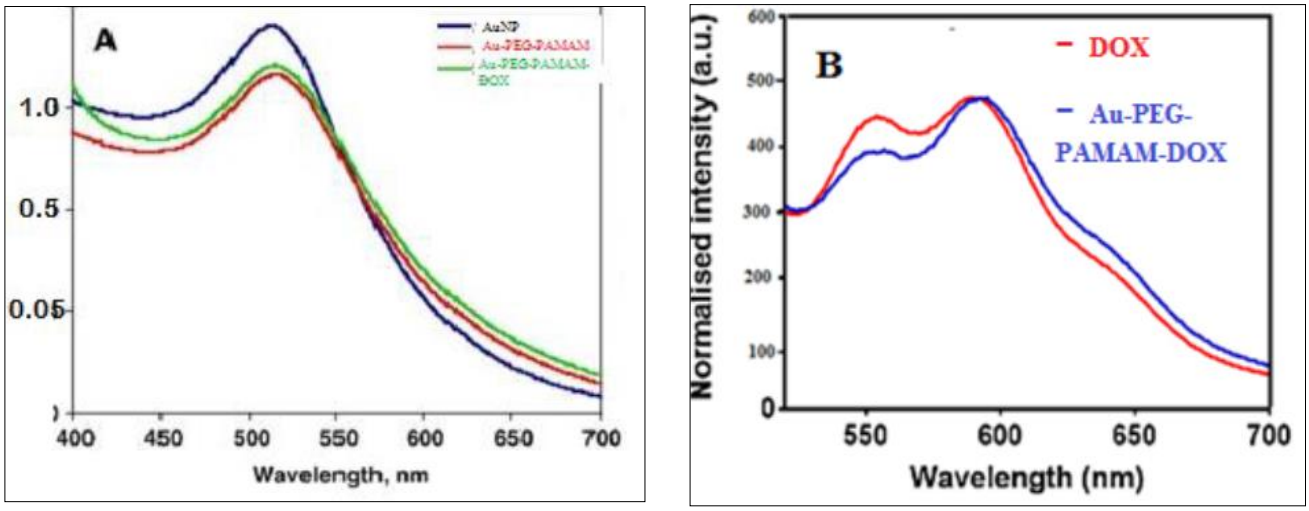

Figure 1 (A) demonstrates the ultraviolet and visible absorption spectra of the $\boldsymbol{Au-PEG-PAMAM-DOX}$ nanosystem as well as it is intermediate product. (B): the fluorescence spectra of DOX and the $\boldsymbol{Au-PEG-PAMAM-DOX}$ nanosystem

In addition, fluorescence spectroscopy was used to characterize the DOX-loaded Nano carriers as well as the DOX solution, and the results were compared to an equivalent DOX concentration of 10 g/ml. The fluorescence of the $Au-PEG-PAMAM-DOX$ nano-system revealed the expected emission band from the DOX, albeit at a reduced intensity when compared to the fluorescence spectra of a free DOX solution (normalized by 1.50 multiplication). This lessening in the fluorescence exhaust intensity of the bound DOX would also lend support to the DOX's effective conjugation to the PAMAM. The red shift that can be detected in the absorbance spectrum can also be seen in the emission spectra of nanocarriers that have been loaded with DOX as can be seen in Figure 1. On the other hand, there is a fall in intensity in the region with lower wavelengths, while there is an increase in intensity in the region with higher wavelengths. These declines may be the result of agglomeration of the nanosystem absorbed in oneself effect nevertheless, are more likely to be caused by the conjugation of the DOX to the PAMAM, which dampens the emission of the DOX [28]. This, in conjunction with the results of the absorption spectroscopy, demonstrates that the DOX molecules were able to successfully bind with the surface of the Au NPs, hence verifying the development of the DOX-loaded nanocarrier. The zeta potential measurement of the specime provided additional proof that the nanocarrier was successfully formed; the values of the zeta potential that were obtained for the $Au-PEG-PAMAM-DOX$ nanosystem at various phases of production are displayed. The zeta potential of $Au-PEG$, which had an average value of 15.0, 0.9 mV before conjugation with Au nanoparticles, became more positive after the conjugation process (average value -35.43, 1.5 mV). The negative charge carried by the gold nanoparticles is shielded and neutralized by the charge-neutral PEG [29]. When Au NPs are coupled with more neutral PEG, the resulting Au-PEG nanoparticle has a positive charge. This is because the negative charge of the Au NPs is converted into a positive charge by the connection. After functionalizing Au-PEG with negatively

charged PAMAM G4 dendrimer, the surface zeta potential altered to an average of (-14.47, 1.32). This shows that the PAMAM dendrimer's carboxylic groups were covalently coupled with the Au-amino PEG's groups via an EDC coupling reaction. The surface zeta potential changed to this value after functionalizing Au-PEG with negatively charged PAMAM G4 dendrimer. The variation in surface zeta potential was measured, which allowed this conclusion to be drawn. It is possible that the DOX medicine was successfully loaded on to the surface of $Au - PEG - PAMAM$ nanoparticles due to the fact that the conjugation of positively charged doxorubicin resulted in changes in the surface zeta potential of $Au - PEG - PAMAMG4 - DOX$ (with an average value of -9.69, 1.30). TEM and SEM were utilized in order to measure the particle size of the $Au - PEG - PAMAM - DOX$ nanosystem. Micrographs taken using TEM and SEM of the nano. Revealed that the nanoparticles' sizes ranged from 15 nm to 20 nm as showed Figure 2.A. The hydrodynamic diameters of each nanoparticle were measured using a technique called dynamic light scattering (DLS). According to the information that is presented, the diameter of each and every nanoparticle measured less than 100 nm on average Figure 2.B, and the values of their PDI spanned the range of 0.5 to 0.7. It has been established that nanoparticles with an average particle size of less than 100 nm are more effective for the goal of passively targeting tumors [29].

There had been no instances of agglomeration at any time during the course of the synthesis; rather, there had been a progressive rise in particle size as a result of the conjugation of PEG and the dendrimer to the system. This had led to the gradual increase in particle size. As can be observed in Figure 2, the absorption band of the nanoparticles did not show any signs of broadening while the experiment was being carried out. When Au NPs were treated with PEG conjugation, an intermolecular hydrogen bond was formed between the water molecule and the conjugated PEG molecule [24]. This prevented the gold nanoparticles from aggregating into larger clusters. The hydrophilicity of the treated Au NPs was able to be increased, which allowed this goal to be achieved. Dendrimers were incorporated into the formulation so that they could assist in the stability of the nanoparticles and prevent agglomeration [30]. The Nano system was totally dispersed in water, and it did not exhibit any evidence of agglomeration. This was corroborated by the system's persistent dispensability, which indicated that there was no aggregation. The TEM and SEM clearly demonstrated this point.

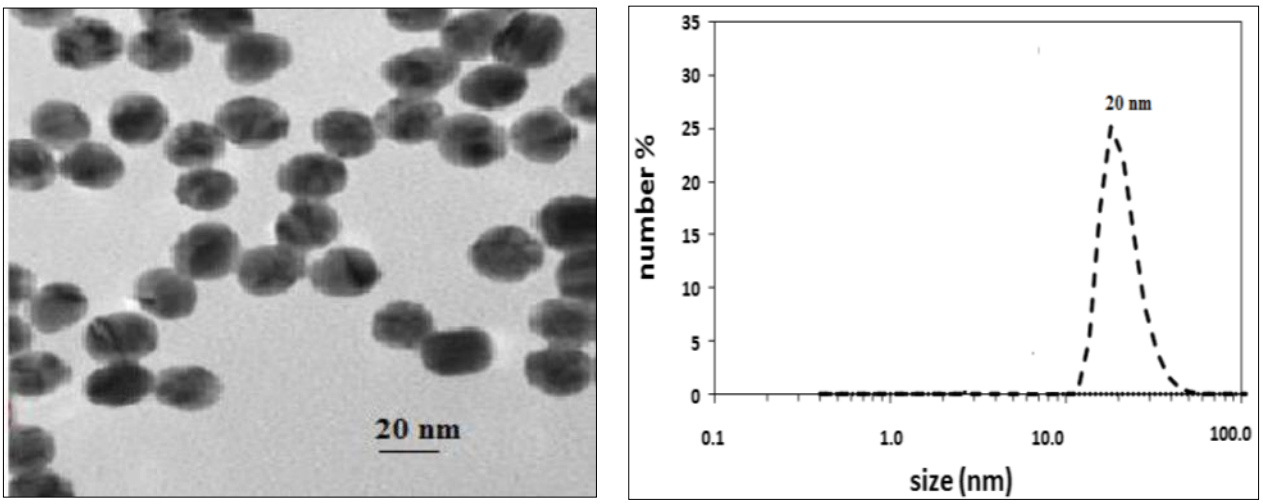

Figure 2 (A). TEM images of Au nanoparticles of averaged diameter 20 nm, (B) DLS spectra showing particle sizes of 20 nm

3.2 Acellular DOX release

Controlling the release of the payload (drug) is the ultimate objective of any nanocarrier, the kinetics of the drug delivery system based on $Au - PEG - PAMAM - DOX$ were studied through the use of a dialysis technique. In order to simulate cellular lysosomal compartments *In vitro* , the nanosystem was incubated in a buffer solution with a physiological pH (pH 7.0). Additionally, the nanosystem was treated in an acidic buffer solution (pH 4.0). The time-dependent DOX release curves of $Au - PEG - PAMAM - DOX$ at pH 7.0 and pH 4.0 are depicted in Figure 2. There was no discernible DOX leakage from the $Au - PEG - PAMAM - DOX$ compound when the pH was 7.0. In contrast, we found that after 96 hours at a pH of 4.0, there was roughly a 50% release of DOX from the Nano system. We suspect that this was caused by the amide bond cleavage that occurred between the DOX and the dendrimer. The data release profile demonstrated that nanoparticles released more drug than conventional particles, and, more crucially, that the drug was released in a regulated way over a period of 96 hours at a pH of 4.0

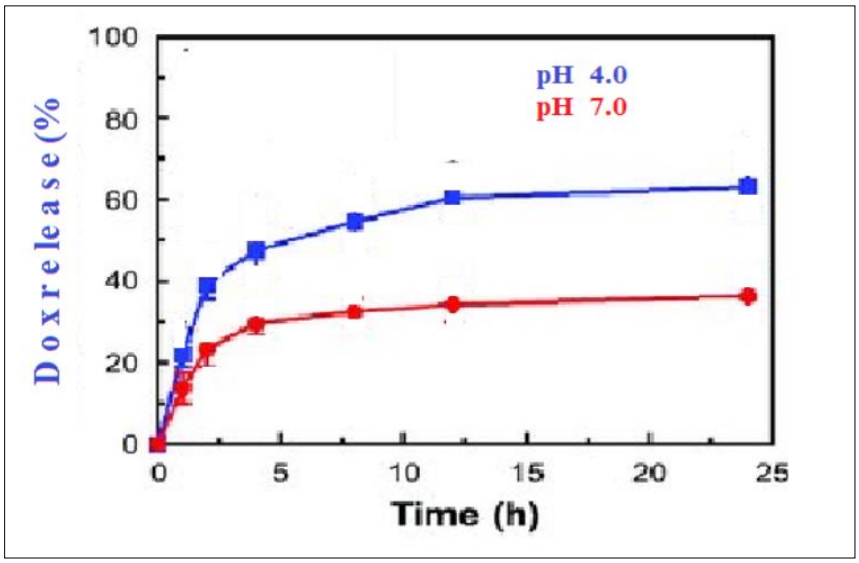

Figure 3 PH dependent release of DOX by in $Au - PEG - PAMAM - DOX$ nanosystem

When measured against a healthy pH of 7.0, the system that was built reveals a substantial amount of untapped Possibility of additional development in certain applications. To acquire a better understanding of the drug release kinetics, the data on drug release were evaluated using a zero order kinetics model at pH 4. The zero order model is more useful for slow drug release kinetics [31]. The equation (2) was used to display the release data against time and assess the release kinetics:

$$Qt = Q0 + K0t\ Eq.2 \ldots.(2)$$

3.3 Cell viability

The MTT assay was utilized to determine the level of cytotoxicity exhibited *In vitro* by free DOX , $Au - PEG - PAMAM$ and $Au - PEG - PAMAM - DOX$. When developing the nanosystem, the components of the $Au - PEG - PAMAM - DOX$ system were employed as a point of reference in order to establish whether or not the entire system was more effective than the free DOX. A total of 48 hours was spent to the A549 cells to each drug at doses ranging from 1.25 g/ml all the way up to 10 g/ml (or DOX equivalent Au concentration). As can be shown in Figure 4.

A total of 48 hours was spent to the A549 cells to each drug at doses ranging from 1.25 g/ml all the way up to 10 g/ml (or DOX equivalent Au concentration). As can be shown in Figure 5, $Au - PEG - PAMAM - DOX$ free DOX, Au NPs, and $Au - PEG - PAMAM$ all displayed dose- and time-dependent cytotoxicity profiles.

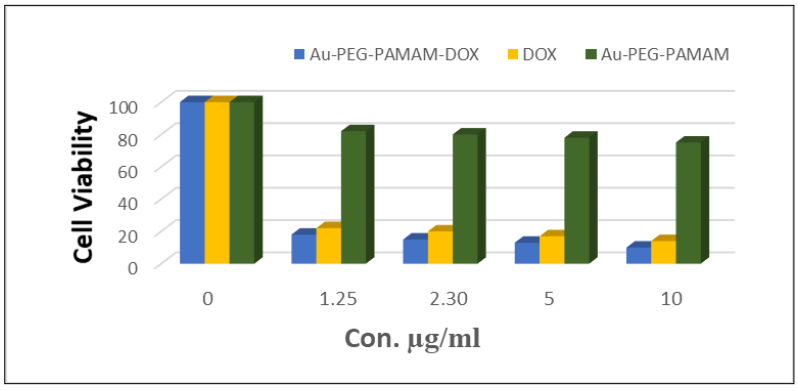

Figure 4 *In vitro* cytotoxicity of A549 cells treated with different concentrations of Au-PEGPAMAM- DOX, free DOX and Au-PEG-PAMAM materials after 24 hr

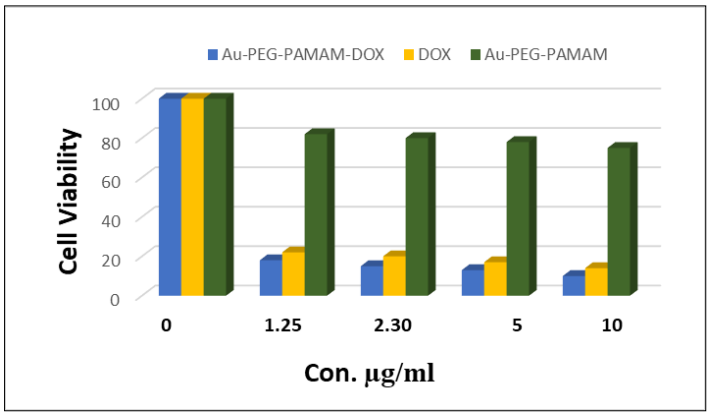

Figure 5 *In vitro* cytotoxicity of A549 cells treated with different concentrations of Au-PEGPAMAM- DOX, free DOX and Au-PEG-PAMAM materials after 48 hr

The Au PEG-PAMAM material was found to have a conjugated PAMAM dendrimer on its surface, and it was this dendrimer that caused the material to statistically significantly lose vitality while only having a little effect on cell viability. [32-33]. The finding that an increase in exposure duration had a negative effect on cell viability was supported by this finding. It is important to notice that the $Au - PEG - PAMAM - DOX$ nanoparticles showed a higher level of cytotoxicity compared to free DOX, Au NPs, and $Au - PEG - PAMAM$ nanoparticles. This finding suggests that the end system boosts the effectiveness of the DOX. In comparison, the free DOX produced an IC 50 of 0.39 µg/ml while the $Au - PEG - PAMAM - DOX$ produced an IC 50 of 0.28 µg/ml after being exposed for 48 hours. For $Au - PEG - PAMAM$ the IC50 was 12 µg/ml. Even though the differences in viability levels were not as noticeable after longer exposures, the results indicate the development of the nanocarrier system could dramatically modify the rate at which the DOX destroys the cell. This is evidenced by the varying IC 50 values in the less than 48-hour exposures.

3.4 *In vitro* confocal imaging

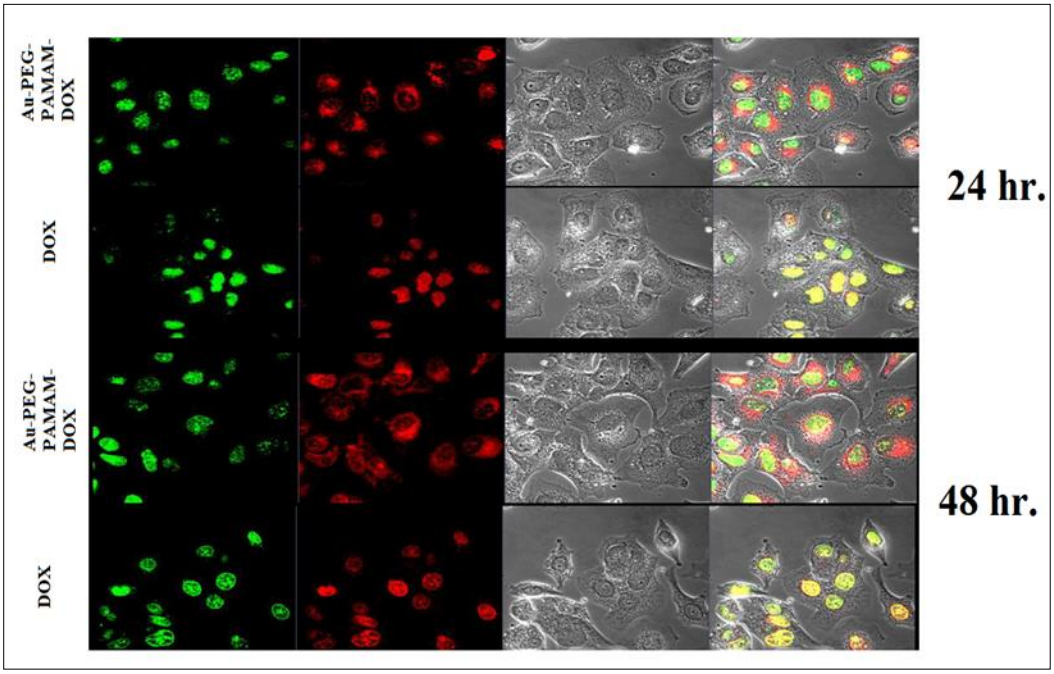

Figure 6 Employing an $\boldsymbol{Au - PEG - PAMAM - DOX}$ Nanosystem, Materials were fixed with formalin, washed, and treated with A549 cells for 24, and 48 hours

As can be seen in Figure 6, With the use of CLSM and counterstaining the nuclei of A549 cells, the process of monitoring drug release and accumulation *In vitro* was completed. This was done so that the results could be analyzed. Following the DOX emission made it possible to observe not just where the DOX was accumulating but also where it was being produced. PEGylated dendrimer nanoparticles have been shown to be internalized into cells by an EPR effect and to

reside outside of the nucleus, most likely in the lysosomal compartments of the cell [34]. This was discovered through a series of experiments in which the nanoparticles were subjected to magnetic fields. As can be seen in Figure 6, following a 48 hr. incubation with the $Au - PEG - PAMAM - DOX$ Nano system, the drug had collected in the lysosomal partitions of the cells as shown by the red fluorescence emitted by DOX. This was observed. These findings lend credence to the hypothesis that we have developed a pH - sensitive release system for DOX. This hypothesis is also supported by the results of the investigation in to the acellular release of DOX, which demonstrated that the medication was liberated from the nanosystem when the pH was adjusted to 4.0. (Fig. 6). As illustrated in Figure 6, the red fluorescence emitted by DOX could be observed in both the cytoplasm and the cell nucleus after the incubation period was prolonged to a total of 48-hours. It first went into the cytoplasm, where it accumulated in the lysosomes; then, after a period of 48 hours, there was a release of the drug from the lysosomes, and it went into the nucleus of the cell. These data demonstrate beyond a reasonable question that the Au-PEG-PAMAM-DOX Nano system did, in fact, release the DOX in a controlled manner.

4 Conclusion

Nanosystem comprised of DOX and Au NPs , $Au - PEG - PAMAM - DOX$ In comparison to the citrate polymer coated Au, the PEG polymer coated Au NPs displayed increased levels of colloidal stability and surface area. minimal levels of toxicity while maintaining biocompatibility. The active ingredient DOX was conjugated on to the completed system with the assistance of a dendrimer and an amide bond. Because the nano carrier was shown to enter the cell via a distinct mechanism and accumulate in the lysosomal compartments (pH 4-5) of the cells, the pH- sensitive drug release that was demonstrated by the final drug delivery system $Au - PEG - PAMAM - DOX$ was later confirmed in *In vitro* tests. This was done because the pH-sensitive drug release was demonstrated by the final drug delivery system. The Au-PEG-PAMAM-DOX Nanoparticle, which had DOX loaded onto it, caused a shift in the manner in which DOX was taken up by cells. This, in turn, had an effect on the cytotoxicity that was associated with DOX and improved the DOX's effectiveness when used in short-term exposures. The $Au - PEG - PAMAM - DOX$ nanosystem is an unique multifunctional dendrimer-based nanosystem that may offer a new platform for the intracellular release of anticancer drugs at tumor locations.

Compliance with ethical standards

Acknowledgments

I am grateful to all of those with whom I have had the pleasure to work during this and other related projects.

Disclosure of conflict of interest

The authors have no conflicts of interest to declare.

References

[1] Plummer M, de Martel C, Vignat J, et al. Global burden of cancers attributable to infections in 2012: a synthetic analysis. Lancet Glob Health. 2016, 4:e609–e616. [Crossref], [PubMed], [Web of Science ®], [Google Scholar]

[2] Haga A, Takahashi W, Aoki S, et al. Classification of early stage non-small cell lung cancers on computed tomographic images into histological types using radiomic features: interobserver delineation variability analysis. Radiol Phys Technol. 2018, 11:27–35. [Crossref], [PubMed], [Web of Science ®], [Google Scholar]

[3] Mokhtari RB, Homayouni TS, Baluch N, et al. Combination therapy in combating cancer. Oncotarget 2017, 8:38022. [Crossref], [PubMed], [Google Scholar]

[4] Chakraborty S, Rahman T. The difficulties in cancer treatment. Ecancermedicalscience. 2012, 6:ed16. [PubMed], [Google Scholar]

[5] Kleinstreuer C, Feng Y, Childress E. Drug-targeting methodologies with applications: a review. World J Clin Cases. 2014, 2:742–756. [Crossref], [PubMed], [Web of Science ®], [Google Scholar]

[6] Jha RK, Jha PK, Chaudhury K, et al. An emerging interface between life science and nanotechnology: present status and prospects of reproductive healthcare aided by nano-biotechnology. Nano Rev 2014, 5:10. [Google Scholar]

[7] Mody VV, Siwale R, Singh A, et al. Introduction to metallic nanoparticles. J Pharm Bioallied Sci. 2010, 2:282–289. [Crossref], [PubMed], [Google Scholar]

[8] Shankar SS, Rai A, Ahmad A, et al. Rapid synthesis of Au, Ag, and bimetallic Au core–Ag shell nanoparticles using Neem (Azadirachta indica) leaf broth. J Colloid Interface Sci. 2004, 275:496–502. [Crossref], [PubMed], [Web of Science ®], [Google Scholar]

[9] Cai W, Gao T, Hong H, et al. Applications of gold nanoparticles in cancer nanotechnology. Nanotechnol Sci Appl. 2008, 1:17–32. [Taylor & Francis Online], [Google Scholar]

[10] Geetha R, Ashokkumar T, Tamilselvan S, et al. Green synthesis of gold nanoparticles and their anticancer activity. Cancer Nano. 2013, 4:91–98. [Crossref], [PubMed], [Google Scholar]

[11] Tian, F., Bonnier, F., Casey, A., Shanahan, A. E., & Byrne, H. J. (2014). Surface enhanced Raman scattering with gold nanoparticles: effect of particle shape. Analytical Methods, 6(22), 9116-9123. https://doi.org/10.1039/C4AY02112F.

[12] Dreaden, E. C., Austin, L. A., Mackey, M. A., & El-Sayed, M. A. (2012). Size matters: gold nanoparticles in targeted cancer drug delivery. Therapeutic delivery, 3(4), 457-478. https://doi.org/10.4155/tde.12.21.

[13] Liu, L., Tang, Y., Dai, S., Kleitz, F., & Qiao, S. Z. (2016). Smart surface-enhanced Raman scattering traceable drug delivery systems. Nanoscale, 8(25), 12803-12811. https://doi.org/10.1039/C6NR03869G.

[14] Zong, S., Wang, Z., Chen, H., Yang, J., & Cui, Y. (2013). Surface enhanced Raman scattering traceable and glutathione responsive nanocarrier for the intracellular drug delivery. Analytical chemistry, 85(4), 2223-2230. https://doi.org/10.1021/ac303028v.

[15] Lee, K. Y., Wang, Y., & Nie, S. (2015). In vitro study of a pH-sensitive multifunctional doxorubicin–gold nanoparticle system: Therapeutic effect and surface enhanced Raman scattering. RSC Advances, 5(81), 65651-65659. https://doi.org/10.1039/C5RA09872F.

[16] Zhong, Y., Wang, C., Cheng, R., Cheng, L., Meng, F., Liu, Z., & Zhong, Z. (2014). cRGD-directed, NIR-responsive and robust AuNR/PEG–PCL hybrid nanoparticles for targeted chemotherapy of glioblastoma in vivo. Journal of Controlled Release, 195, 63-71. https://doi.org/10.1016/j.jconrel.2014.07.054.

[17] Moustaoui, H., Movia, D., Dupont, N., Bouchemal, N., Casale, S., Djaker, N., .. & Spadavecchia, J. (2016). Tunable design of Gold (III)–Doxorubicin Complex–PEGylated nanocarrier. The golden doxorubicin for oncological applications. ACS applied materials & interfaces, 8(31), 19946-19957. https://doi.org/10.1021/acsami.6b07250.

[18] Gao, J., Huang, X., Liu, H., Zan, F., & Ren, J. (2012). Colloidal stability of gold nanoparticles modified with thiol compounds: bioconjugation and application in cancer cell imaging. Langmuir, 28(9), 4464-4471. https://doi.org/10.1021/la204289k.

[19] Lazarovits, J., Chen, Y. Y., Sykes, E. A., & Chan, W. C. (2015). Nanoparticle–blood interactions: the implications on solid tumour targeting. Chemical Communications, 51(14), 2756-2767. https://doi.org/10.1039/C4CC07644C.

[20] Jokerst, J. V., Lobovkina, T., Zare, R. N., & Gambhir, S. S. (2011). Nanoparticle PEGylation for imaging and therapy. Nanomedicine, 6(4), 715-728. https://doi.org/10.2217/nnm.11.19.

[21] Lane, L. A., Qian, X., Smith, A. M., & Nie, S. (2015). Physical chemistry of nanomedicine: understanding the complex behaviors of nanoparticles in vivo. Annual review of physical chemistry, 66, 521-547. https://doi.org/10.1146/annurev-physchem-040513-103718.

[22] Bugno, J., Hsu, H. J., & Hong, S. (2015). Recent advances in targeted drug delivery approaches using dendritic polymers. Biomaterials science, 3(7), 1025-1034. https://doi.org/10.1039/C4BM00351A.

[23] Kurniasih, I. N., Keilitz, J., & Haag, R. (2015). Dendritic nanocarriers based on hyperbranched polymers. Chemical Society Reviews, 44(12), 4145-4164. https://doi.org/10.1039/C4CS00333K.

[24] Zhang, W. L., Li, N., Huang, J., Yu, J. H., Wang, D. X., Li, Y. P., & Liu, S. Y. (2010). Gadolinium-conjugated FA-PEG-PAMAM-COOH nanoparticles as potential tumor-targeted circulation-prolonged macromolecular MRI contrast agents. Journal of applied polymer science, 118(3), 1805-1814. https://doi.org/10.1002/app.32494.

[25] He, H., Li, Y., Jia, X. R., Du, J., Ying, X., Lu, W. L., .. & Wei, Y. (2011). PEGylated Poly (amidoamine) dendrimer-based dual-targeting carrier for treating brain tumors. Biomaterials, 32(2), 478-487. https://doi.org/10.1016/j.biomaterials.2010.09.002.

[26] Huang, F., Watson, E., Dempsey, C., & Suh, J. (2013). Real-time particle tracking for studying intracellular trafficking of pharmaceutical nanocarriers. Cellular and Subcellular Nanotechnology: Methods and Protocols, 211-223. https://doi.org/10.1007/978-1-62703-336-7_20 .

[27] Li, X., Takashima, M., Yuba, E., Harada, A., & Kono, K. (2014). PEGylated PAMAM dendrimer–doxorubicin conjugate-hybridized gold nanorod for combined photothermal-chemotherapy. Biomaterials, 35(24), 6576-6584. https://doi.org/10.1016/j.biomaterials.2014.04.043.

[28] Venkatesan, R., Pichaimani, A., Hari, K., Balasubramanian, P. K., Kulandaivel, J., & Premkumar, K. (2013). Doxorubicin conjugated gold nanorods: a sustained drug delivery carrier for improved anticancer therapy. Journal of Materials Chemistry B, 1(7), 1010-1018. https://doi.org/10.1039/C2TB00078D.

[29] Ganta, S., Devalapally, H., Shahiwala, A., & Amiji, M. (2008). A review of stimuli-responsive nanocarriers for drug and gene delivery. Journal of controlled release, 126(3), 187-204. https://doi.org/10.1016/j.jconrel.2007.12.017.

[30] Iacovita, C., Stiufiuc, R., Radu, T., Florea, A., Stiufiuc, G., Dutu, A., .. & Lucaciu, C. M. (2015). Polyethylene glycol-mediated synthesis of cubic iron oxide nanoparticles with high heating power. Nanoscale research letters, 10(1), 1-16. https://doi.org/10.1186%2Fs11671-015-1091-0.

[31] Crooks, R. M., Zhao, M., Sun, L., Chechik, V., & Yeung, L. K. (2001). Dendrimer-encapsulated metal nanoparticles: synthesis, characterization, and applications to catalysis. Accounts of chemical research, 34(3), 181-190. https://doi.org/10.1021/ar000110a.

[32] Golshan, M., Salami-Kalajahi, M., Roghani-Mamaqani, H., & Mohammadi, M. (2017). Poly (propylene imine) dendrimer-grafted nanocrystalline cellulose: Doxorubicin loading and release behavior. Polymer, 117, 287-294. https://doi.org/10.1016/j.polymer.2017.04.047.

[33] Gürbüz, M. U., Öztürk, K., Ertürk, A. S., Yoyen-Ermis, D., Esendagli, G., Çalış, S., & Tülü, M. (2016). Cytotoxicity and biodistribution studies on PEGylated EDA and PEG cored PAMAM dendrimers. Journal of Biomaterials science, Polymer edition, 27(16), 1645-1658. https://doi.org/10.1080/09205063.2016.1226044.

[34] Wolinsky, J. B., & Grinstaff, M. W. (2008). Therapeutic and diagnostic applications of dendrimers for cancer treatment. Advanced drug delivery reviews, 60(9), 1037-1055. https://doi.org/10.1016/j.addr.2008.02.012.